The Elementary Cellulose Fibril in *Picea abies*: Comparison of Transmission Electron Microscopy, Small-Angle X-ray Scattering, and Wide-Angle X-ray Scattering Results

H. F. Jakob,[†] D. Fengel,[‡] S. E. Tschegg,[§] and P. Fratzl*,[†]

Institut für Festkörperphysik der Universität Wien, Strudlhofgasse 4, A-1090 Wien, Austria, Institut für Holzforschung der Universität München, Winzererstrasse 45, 80797 München, Germany, and Institut für Meteorologie und Physik der Universität für Bodenkultur, Türkenschanzstrasse 18, A-1180 Wien, Austria

Received April 14, 1995; Revised Manuscript Received September 25, 1995[⊗]

ABSTRACT: The wood cell wall is built with elementary cellulose fibrils (ECF) having a uniform thickness of 25 ± 2 Å. This was shown by investigating the same samples independently with three different experimental techniques, transmission electron microscopy (TEM), wide-angle X-ray scattering (WAXS), and small-angle X-ray scattering (SAXS). Discrepancies between results from these techniques discussed in many earlier studies did not appear in the present work. In particular, it was shown that the size distribution measured on TEM pictures is exactly the same as the one estimated from SAXS, if the statistical error introduced by the grain size of the contrasting medium is taken into account for the evaluation of the pictures. The fact that native cellulose fibrils have a uniform thickness in the wood cell wall—which is not the case in many other cellulose preparations—could indicate a biological regulation of the thickness, possibly to achieve better mechanical stability of the cell wall.

1. Introduction

The existence of an elementary cellulose fibril (ECF) as the structural unit of the main cell wall layer (S_2) of the tracheids in *Picea abies* was proposed a long time ago.[1,2] Since then, the size of the smallest crystalline units has been measured in cellulose from various origins by transmission electron microscopy (TEM), wide-angle X-ray scattering (WAXS), and small-angle X-ray scattering (SAXS). A collection of data is given in Table 1.

It is evident from these data that the size of these crystalline regions shows a great variability. In some cases this was interpreted as being due to the agglomeration of elementary subunits of about 35 Å in size,[3] and in other cases this interpretation was refuted and the existence of an ECF questioned altogether.[4]

For native cellulose fibrils in wood cell walls, however, the distribution of fibril diameters was more consistently peaked at a value between 25 and 35 Å (see Table 2). In particular, recent SAXS measurements in sprucewood (*Picea abies*) revealed a very narrow distribution of fibril diameters (4.4 Å) centered at 25 Å,[5] thus confirming the idea of ECF's—at least in the wood cell wall of *Picea abies*. This was in marked contrast to a previous TEM study on the same type of material,[6] where a much broader distribution of fibril diameters (centered at about 24 Å, but with a full width at half-maximum about 13 Å) was measured.

In order to clarify the situation, we have undertaken a parallel investigation using TEM, WAXS, and SAXS applied to the same samples taken from earlywood of *Picea abies*. Although all three methods have been used before to investigate the size of cellulose fibrils (see Tables 1 and 2), each of these methods is expected to give a slightly different type of information. Indeed, TEM has the advantage of providing direct pictures but requires a serious chemical treatment of the samples (delignification, dehydration, embedding, and staining). This sample preparation can be completely avoided with the two scattering techniques, WAXS and SAXS, where native samples can be investigated. Obtaining good statistics for the fibril diameter is another difficulty of TEM, because a great number of pictures have to be evaluated quantitatively. Since both scattering methods average inherently over the structures inside a macroscopic sample volume, say a cubic millimeter, good statistics are automatically obtained there. The main drawback of SAXS and WAXS is that they are indirect methods and that one has to rely on models to evaluate the data. Moreover, the width of Bragg peaks in X-ray scattering depends not only on the size of the crystalline regions but also on their perfection, which has to be considered carefully when interpreting WAXS results. This problem does not arise with SAXS, where crystal imperfection does not influence the results.

Finally, it also should be kept in mind that the contrast in TEM is due to negative staining, in WAXS to the crystalline structure of the fibrils, and in SAXS to the electron density contrast with the surrounding matrix. A comparison of results with all three methods is reported in this paper, together with a critical reevaluation of current models concerning the existence, size, and structure of elementary cellulose fibrils in the wood cell wall.

2. Materials and Methods

For all investigations (SAXS, WAXS, and TEM) we used normal, air-dried sprucewood samples (*Picea abies*). Slices were cut out of a normal part of the stem, i.e., without resin canals, without any knots, and without reaction wood. The slices were cut along the longitudinal direction of the stem. In particular, tangential sections were taken out of the earlywood part of an annual ring. In such samples, the elementary cellulose fibrils are running practically parallel to the longitudinal direction of the stem.[5]

Since scattering measurements do not require any chemical or physical treatment, the wood samples were

* To whom correspondence should be addressed; e-mail: fratzl@pap.univie.ac.at.
[†] Institut für Festkörperphysik der Universität Wien.
[‡] Institut für Holzforschung der Universität Munchen.
[§] Institut für Meteorologie und Physik der Universität für Bodenkultur, Wien.
[⊗] Abstract published in *Advance ACS Abstracts,* November 1, 1995.

0024-9297/95/2228-8782$09.00/0

Table 1. Summary of the Fibril Diameter Measured in Various Types of Cellulose[a]

authors	method	diameter of fibrils in cellulose (Å)					
		valonia	bacteria	cotton	flax	jute	ramie
Heyn, 1955[1]	SAXS			55	28	28	43
Scallan, 1971[18]	chemical	33	31				33
Hindeleh, 1972[19]	WAXS						50
Haase et al., 1973, 1974[20,21]	WAXS	105	84				52
	SAXS		60–180				50–400
Blackwell and Kolpak, 1975[3]	WAXS						
Boylston and Hebert, 1980[22]	EM	107	53	22			25
	WAXS	112	55	40			44
Nishimura et al., 1982[23]	WAXS						
Fink et al., 1985[17]	WAXS						
Fink et al., 1990[4]	WAXS	90–100	50–60				50
	TEM	100–350	70–90				100–150
Fengel et al.[24]	WAXS			35–60			

[a] The table is not meant to be exhaustive.

Table 2. Summary of Cellulose Fibrils inside the Wood Cell Wall of Several Species According to Different Authors

authors	cellulose fibrils in the wood cell wall		
	method	type of wood	diameter (Å)
Heyn, 1969[13]	TEM	Pinus caribea	35
Scallan, 1971[18]	chemical	?	27
Normura and Yamada, 1972[25]	WAXS	Akamatsu	28
Fengel, 1978[6]	TEM	Picea abies	15–50
Nishimura et al., 1982[23]	WAXS	Akamatsu	31
Jakob et al., 1994[5]	WAXS	Picea abies	25
this work	WAXS	Picea abies	25
	WAXS		19–22
	TEM		25

investigated in their natural state by SAXS and WAXS. All specimens had the same thickness of 200 μm and were encapsulated in a plastic foil of 100 μm in total thickness in order to prevent drying in the high vacuum of the X-ray apparatus. The longitudinal direction of the samples (i.e. the direction of the stem axis) was perpendicular to the incoming X-ray beam. Scattering patterns were collected with a typical time of 0.5 h per spectrum to provide sufficient counting statistics. The scattering intensity $I(\vec{q})$ was corrected for the occurring background scattering. $\vec{q}$ is the scattering vector with modulus $q = |\vec{q}| = (4\pi/\lambda) \sin \theta$, and 2θ is the angle between the incoming and the scattered X-ray beam.

The experimental setup consisted of a 12 kW rotating-anode X-ray generator used in a point-focus geometry. The incoming X-ray beam had a circular cross section of 0.6 mm in diameter. The radiation wavelength was $\lambda = 1.54$ Å, corresponding to Cu Kα radiation in combination with a Ni filter. The spectra were taken with a two-dimensional position-sensitive detector (Fa. Siemens) with a sample to detector distance of 21 cm (SAXS) and 7.5 cm (WAXS). Further WAXS measurements were carried out with a $\theta-2\theta$ goniometer.

As for the TEM measurements, the preparation method was more complicated.[7,8] We took the same slices that were used for scattering measurements, which experienced neither physical nor chemical destruction during this first investigation process, and treated them as shown in Figure 1. To emphasize the structural basis of the cells, i.e., the cellulose chains, it was necessary to perform a delignification process with sodium chlorite at several temperatures, 50–70 °C.[9] This was carried out in three steps lasting about 5 h each. After washing, the samples were taken through a dehydration series with ethanol of four steps. For the ultramicrotomy, the specimens were embedded in an

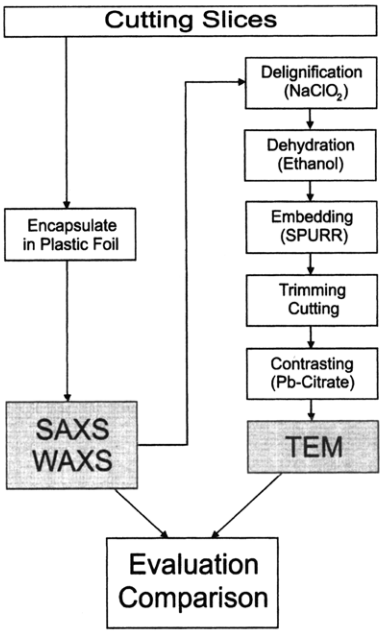

Figure 1. Schematic representation of sample preparation for SAXS, WAXS, and TEM.

epoxy resin (Spurr's medium[10]). After a drying process at 70 °C for about 10 h, sections of about 800–1000 Å in thickness were cut out and picked up onto copper grids bearing a collodion film. Finally, to achieve a better contrast, we treated the sections with lead citrate, which increased the contrast among the elementary cellulose fibrils. The specimens were then examined in an EM10C (Fa. Zeiss).

3. Results

First, X-ray scattering spectra were obtained with a sample to detector distance of 21 cm (SAXS) and 7.5 cm (WAXS). Examples are shown in Figure 2a and 2b, respectively. As visible in Figure 2a, the SAXS spectrum from earlywood consists of a streak in the direction perpendicular to the longitudinal direction of the stem. These data were used to determine the diameter of ECF,[5] i.e., by fitting the function

$$I(q) \approx I_0 \left(4 \frac{J_1\left(\frac{q}{2}D\right)}{qD} \right)^2 + \mathrm{Bgr} \qquad (1)$$

to the scattering intensity, $I(q)$, measured along the streak in Figure 2a. J_1 is the Bessel function of the first kind, I_0 and Bgr being a normalization constant and a

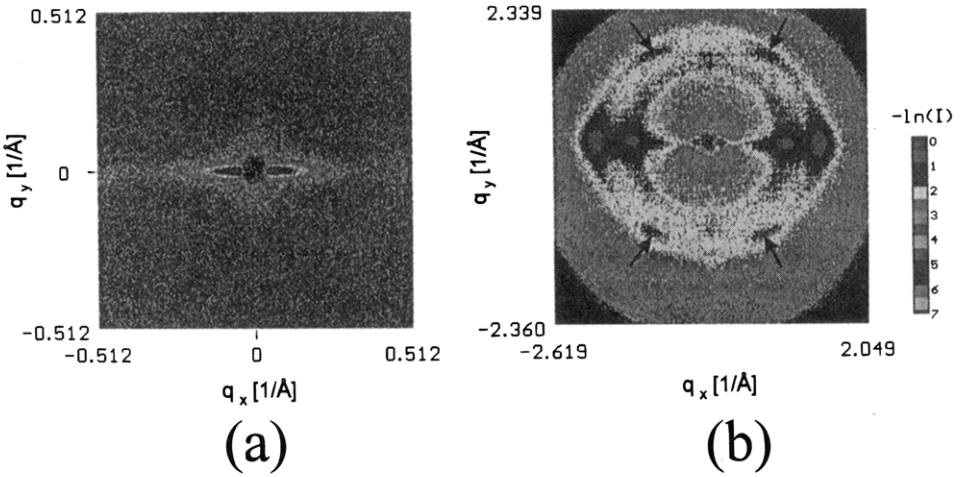

Figure 2. Two-dimensional scattering pictures as obtained in (a) SAXS and (b) WAXS measurements on earlywood of *Picea abies*. The longitudinal direction (corresponding to the stem axis) was vertically oriented.

background, respectively. The position of the first minimum of $I(q)$ then uniquely defines the fibril diameter D, which is found as previously[5] very close to 25 Å.

It is well known that voids are present even in dense regions of wood and contribute to the SAXS. However, we also examined samples with different contents of water to assess the importance of that effect. We found that there is only a substantial contribution to the SAXS intensity due to voids at $q \leq 0.13$ Å^{-1}. Since we determine the size of the fibrils by evaluating the scattering intensity in the region around the minimum of eq 1 around $q \approx 0.3$ Å^{-1}, we think that the scattering from voids will not influence that result. Moreover, the streaks ascribed to the SAXS from cellulose fibrils are tilted by 20° with respect to the equatorial direction in latewood.[5] Since the same tilting is observed for the (020) reflection from cellulose, it would be surprising, if these streaks were due to voids.

The WAXS patterns, on the other hand (Figure 2b), show rings as well as superimposed dots from the crystalline regions of native cellulose. The (110) ($2\theta = 14.8°$) and the ($1\bar{1}0$) reflections ($2\theta = 16.6°$) can be seen on a horizontal line through the center of the picture. Their positions are very close so that they are merged together to a single broad spot. The (020) reflection ($2\theta = 22.7°$) is the strongest of all and can also be seen on the horizontal line. The four diffraction spots marked by arrows correspond to the (012) reflection ($2\theta = 20.6°$). Note that we have indexed the reflections according to the monoclinic two-chain unit cell of Gardner and Blackwell[11] (c axis of the unit cell parallel to the fiber axis). The small-angle part (Figure 2a) of the spectrum is now only visible as a tiny streak in the center of Figure 2b.

The average size of the cellulose crystallites in directions orthogonal to the (110), ($1\bar{1}0$), (012), and (020) planes was determined using the Scherrer equation[12]

$$d_{\text{Scherrer}} = \frac{2(3 \ln 2)^{1/2} \lambda}{\pi \text{FWHM}_{2\theta} \cos \theta} \qquad (2)$$

where λ is the wavelength of the X-ray beam, 2θ the scattering angle, and $\text{FWHM}_{2\theta}$ the full width at half maximum of the reflection in the radial direction. Note that the Bragg reflections may be broadened not only by the finite size of the crystallites but also by possible imperfections in the crystal lattice. The evaluation in eq 2 completely neglects such lattice defects, so that

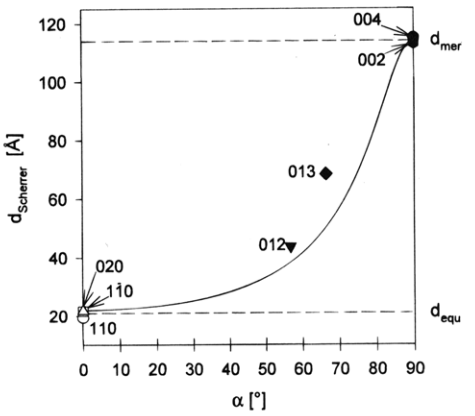

Figure 3. Average size of the cellulose crystallites in the equatorial (d_{equ}, white symbols) and meridional directions (d_{mer}, black symbols) determined using the Scherrer equation (eq 2). For the other reflections, d_{Scherrer} is a combination of both dimensions d_{equ} and d_{mer}, given by $d_{\text{Scherrer}}^{-2} = d_{\text{equ}}^{-2} \cos^2 \alpha + d_{\text{mer}}^{-2} \sin^2 \alpha$ (solid curve).

d_{Scherrer} can be considered as a lower bound for the size of the crystallites only.

Additional WAXS measurements were performed using a diffractometer. The widths of the Bragg reflections were measured along the radial direction for a number of reflections on the equator, i.e., perpendicular to the fibrillar axis, and on the meridian and in between. The peaks were fitted in a narrow region around the maximum using a Gaussian function on a linear background to correct for the amorphous or noncellulosic regions. In cases where two close (i.e., overlapping) reflections could not be resolved (e.g., the (110) and the ($1\bar{1}0$) reflections), we have fixed the predicted positions of the peaks (assuming the unit cell given in Fengel and Wegener[14]) and determined height and width by the fitting procedure.

The obtained width $\text{FWHM}_{2\theta}$ of the Gaussian function was corrected for instrumental broadening, which was also assumed to be Gaussian. The latter correction, however, turned out to be negligible. The corresponding values for d_{Scherrer}, obtained via eq 2, are given in Figure 3.

The values of d_{Scherrer} for all reflections along the equatorial direction, (110), ($1\bar{1}0$), and (020), are almost identical and close to 22 Å. Hence the size of the crystalline region in this direction is $d_{\text{equ}} \approx 22$ Å. The meridional reflections, (002) and (004), both agree with

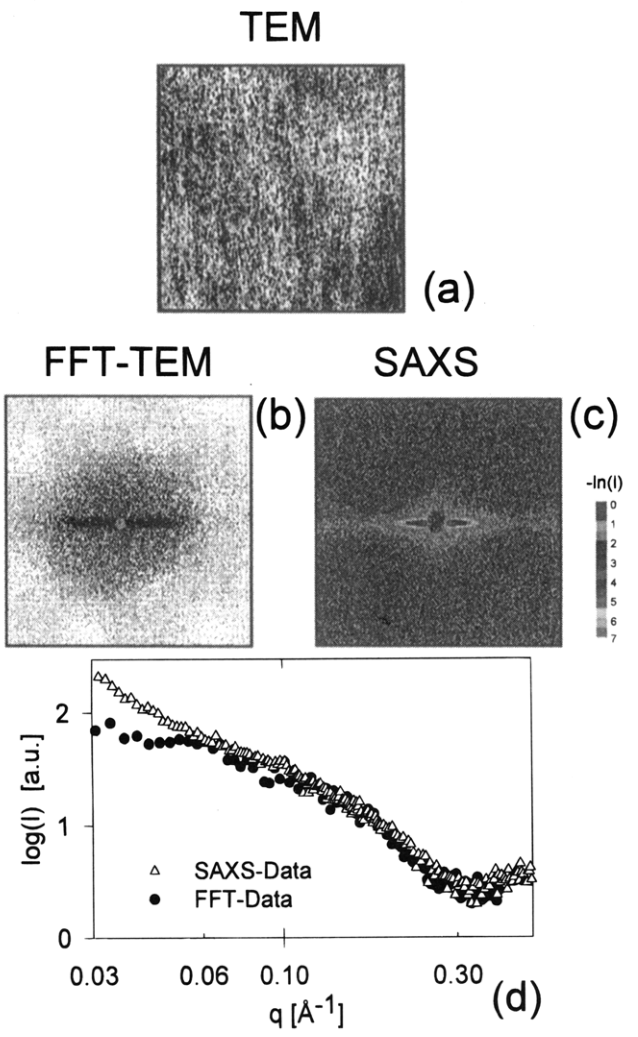

Figure 4. Evaluation and comparison of TEM and SAXS measurements: (a) TEM picture of a part of the S_2 cell wall layer, where the fibrils and the contrasting medium are shown in white and black, respectively; (b) density plot of the squared FFT computed with eq 3 using a digitized version of (a); (c) corresponding 2D SAXS pattern measured with the same sample; (d) comparison of the two intensity distributions obtained by slice integration along the streaks in (b) and (c). The intensities were normalized with an arbitrary multiplicative factor to get an overlap of the two curves at $q = 0.2$ Å.

a meridional extension of the crystalline region $d_{mer} \approx$ 110 Å.

For the other reflections $d_{Scherrer}$ is a combination of both dimensions d_{equ} and d_{mer}. Since there is a considerable angular distribution of the fiber direction even in earlywood (~5°),[5] we estimate that $d^{-2}_{Scherrer} = d^{-2}_{equ} \cos^2 \alpha + d^{-2}_{mer} \sin^2 \alpha$, where α is the angle of the peak off the equatorial direction, as in the case of a powder spectrum. This function is given by the solid curve in Figure 3 and shows good agreement with all the measured data.

A typical result of the TEM investigation is shown in Figure 4a, corresponding to a longitudinal section of a tiny part of the S_2 layer of delignified sprucewood at a magnification of ×220 000. One can clearly see the smallest fibrillar cellulose units (ECF), running in the longitudinal direction and arranged in parallel arrays.[13,14] The dark parts in the figure correspond to the contrasting medium, which is mainly embedded between the ECF's. When we directly measure an average value of the thickness of the ECF's, we get reasonable agreement with SAXS data ($D \approx 25$ Å).

In a previous work, Fengel[6] had measured with high statistical accuracy the distribution of fibril diameters in delignified sprucewood (see Figure 5a). In his diagrams he found a rather broad distribution, but nevertheless an accumulation point at $D \approx 25$ Å. Instead of evaluating TEM pictures by hand as in this earlier work and comparing them with SAXS data, we performed here a direct comparison by means of fast Fourier transformation (FFT). This procedure offers a simple method for evaluating the orientation, size, and arrangement of the ECF's by a procedure similar to the evaluation of SAXS experiments. The TEM pictures (like the one in Figure 4a) were scanned into the computer as a bitmap file. We then transformed these files into (256 × 256) matrices, with only one color level, i.e., 1 for the fibrils and 0 for the contrasting medium in between.

These matrices were then Fourier transformed using the formula

$$b_{m,n} = \frac{1}{N}\sum_{j,k=1}^{N} a_{j,k} \exp\{2\pi i[(j-1)(m-1) + (k-1)(n-1)]/N\} \quad (3)$$

where N is the order of the matrix, and $a_{j,k}$ and $b_{m,n}$ are the terms of the original matrix and its Fourier transform, respectively. For a better comparison with our SAXS measurements we calculated $|b_{m,n}|^2$ and manipulated the resulting list in a way that the zero frequency term appeared in the center of our pictures.

Figure 4b shows the squared Fourier transform of the delignified part of the S_2 cell wall layer (Figure 4a). Figure 4c, on the other hand, shows a real SAXS measurement of the same sprucewood sample. At first sight, both pictures (Figures 4b and 4c) consist qualitatively of a horizontal streak, which is a result of the scattering from the ECF's. For a quantitative comparison of these two pictures, we performed a slice integration along the horizontal streak direction. The so-obtained intensities $I(q)$ were then plotted on a double-logarithmic scale versus q (see Figure 4d), by performing as the only correction a multiplication of $|b_{m,n}|^2$ with a normalization constant chosen to get an overlap of the two curves in Figure 4d around $q \approx 0.2$ Å^{-1}. As one can see, there is good agreement of these two curves above $q = 0.06$ Å^{-1}. In particular, we obtain the same q value for the first minimum, which in turn gives the same size for the mean thickness of the ECF's, i.e., $D =$ 25 Å. The slight disagreement between the intensity curves of TEM and SAXS measurements for values of $q \leq 0.06$ Å^{-1} may be a result of the different dimensions in which the "measurements" were carried out. The Fourier transformation is carried out on a two-dimensional "sample" and compared with a 3D measurement. Another reason may be that air-dried samples contain microcracks that give diffuse X-ray scattering at very small q.[15] In both cases, however, the influence of the artifact is negligible at large q in the region of the first minimum of the intensity curve and so is not expected to have any influence on the determination of the fibril diameter.

4. Discussion

4.1. Comparison of Fibril Diameter: SAXS vs TEM. Cellulose fibrils in the wood cell wall of *Picea abies* were investigated by TEM, SAXS, and WAXS. We have shown (Figure 4) that the squared Fourier transform of the pictures agrees quantitatively with SAXS

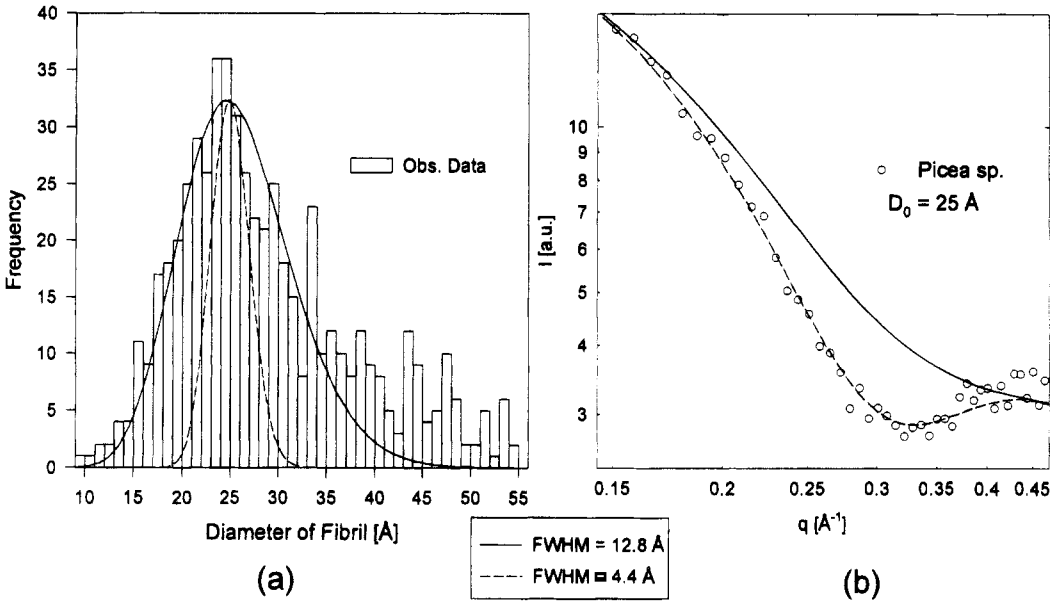

Figure 5. Comparison between the distribution of fibril diameters as measured by TEM and SAXS: (a) distribution of fibril diameter according to Fengel[6] (empty bars); (b) scattering intensity (empty circles) obtained by slice integration of a SAXS measurement (see Figure 3d). The solid curve in (a) shows a fit to the measured fibril diameter distribution for $D \leq 40$ Å using eq 4 and in (b) the transformation of this distribution using eq 5. The dashed curve in (b) shows a fit to the SAXS data using eq 5 and in (a) the corresponding distribution of fibril diameters.

measurements of the same samples. This is exactly what would be expected theoretically. Now the question remains why the distribution of fibril diameters as directly measured on pictures in an earlier study[6] is so much broader than expected from our SAXS results.

First, to quantify this difference, we represent the distribution of the fibril diameters as obtained by Fengel[6] (empty bars in Figure 5a) by a Poisson-like distribution of the form

$$F(D) = \text{const} \times D^{n-1} e^{-n(D/D_0)} \tag{4}$$

where D_0 is the position of the maximum and n is correlated to the full width at half-maximum (FWHM) of the distribution. The solid curve in Figure 5a with FWHM = 12.8 Å is a best fit to the observed data when we only consider data below D = 40 Å. Indeed, the shoulder in the original data may be well due to a clustering of ECF's. To compute the SAXS curve (like the one in Figure 4d) corresponding to this distribution, we used the formula

$$\tilde{I}(q) = \text{const} \times \int F(D) \frac{J_1^2\left(\frac{q}{2}D\right)}{(qD)^2} \, dD \tag{5}$$

where the function $J_1^2(qD/2)/(qD)^2$ corresponds to the SAXS from a single cylindrical fibril.

The solid curve in Figure 5b shows this intensity $\tilde{I}(q)$. This curve does not even have a minimum around $q \approx 0.32$ Å^{-1} and is in contradiction to the observed SAXS data (empty circles in Figure 5b). The dashed curve in Figure 5b represents the best fit to our SAXS data using eqs 4 and 5. Transforming it back into a distribution of fibril diameters, we get the dashed distribution in Figure 5a, which is very narrow (FWHM = 4.4 Å) compared to the observed TEM data.

Knowing that the SAXS measurements are averages over macroscopic sample volumes, while the measurement of an individual fibril thickness in an electron micrograph involves a statistical error in the order of ϵ on each side of the fibril, we expect that the width of the size distribution as measured by TEM, b_{TEM}, must be larger than the one measured by SAXS, b_{SAXS}, by the amount

$$b_{TEM} = (b_{SAXS}^2 + 2\epsilon^2)^{1/2} \tag{6}$$

Here we have approximated all distributions (including the statistical error) as Gaussian functions. With $b_{SAXS} \approx 4.4$ Å and $b_{TEM} \approx 12.8$ Å (see Figure 5), the above equation would be satisfied for $\epsilon \approx 8.5$ Å. Considering that the grain size of the contrasting medium lies between 6 and 10 Å,[6] the estimate with eq 6 simply means that an individual fibril diameter can be measured on an electron micrograph only with a statistical error of the order of magnitude of the grain size of the contrasting medium. This value also corresponds roughly to the distance of two cellulose molecular chains in the cellulose crystallites (~10 Å). Consequently, we think that there is, in fact, no contradiction between the rather broad distribution of fibril diameters measured in TEM micrographs[6] and the existence of an elementary cellulose fibril with a sharply defined diameter as revealed by SAXS.[5] Indeed, the additional statistical error ϵ was completely avoided using the method of Fourier transformation of TEM pictures as discussed in Figure 4.

4.2. Comparison: SAXS vs WAXS. As already discussed, the cell wall in *Picea abies* contains parallel arrays of cellulose fibrils with a uniform diameter of about 25 ± 2 Å, according to SAXS and TEM results. From WAXS results it is well known (see Tables 1 and 2) that cellulose consists of crystalline and disordered regions. In the present case of *Picea abies*, we found that lower bounds for the dimensions of the cellulose crystallites are 22 ± 2 Å in the direction perpendicular to the fibril axis and about 110 ± 4 Å along the axis. This is much smaller than the crystallite dimensions found in many types of cellulose (Table 1) but in reasonable agreement with data on other wood cells, such as those from *Pinus caribea* or *Akamatsu* wood (see

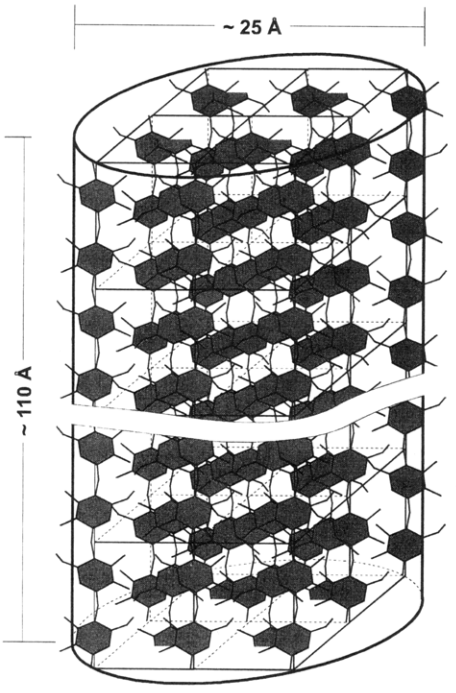

Figure 6. Model for the average crystalline regions in an elementary cellulose fibril derived from SAXS and WAXS measurements. The diameter of the cylinder (thick lines) corresponds to the mean diameter of an ECF, according to the SAXS results. The thin lines represent the monoclinic unit cells of crystalline cellulose (not to scale).

Table 2). Most remarkably, it is also in the same order of magnitude as the fibril diameter as determined by SAXS or TEM.

Our results are summarized in Figure 6. The size of the crystalline regions corresponds to two lattice spacings (boxes in Figure 6) in the plane perpendicular to the fibril axis. Such a crystalline region fits very well inside a cylinder with diameter 25 Å that corresponds to the fibril as measured by SAXS and TEM (see Figure 6). Hence, we may conclude that the crystallites extend over the whole diameter of the cellulose fibril. In the axial direction the size of the crystallites is limited to about 110 Å, which is very short compared to the length of an actual fibril (as seen, e.g., in Figure 4a).

Hence, the fibrillar network of the cell wall layer S_2 is built up of ECF's with uniform diameter, which may occasionally join to form larger units. The inner structure of ECF's consists of cellulose molecular chains with crystalline and amorphous regions alternating along the fibril axis. It is possible that the fibrils are interconnected via molecules attached to the fibrils in these amorphous regions, as proposed, e.g., by Fengel and Wegener.[14] The existence of a uniform diameter for the fibrils does not support, however, the fringed fibrillar model,[16,17] where fibrils join and branch in an irregular manner.

4.3. Conclusion. We have shown that three experimental techniques, TEM, WAXS, and SAXS, yield compatible results for the shape and structure of cellulose fibrils in the S_2 cell wall of *Picea abies*. SAXS shows that there is a uniform fibril diameter of 25 ± 2 Å. WAXS reveals crystalline regions of about the same thickness and with a length along the fibril axis of typically 110 Å. A new analysis of existing[6] as well as new TEM data also shows that TEM and SAXS yield perfectly consistent results regarding the thickness of cellulose fibrils.

This result for *Picea abies* fits well earlier data for native cellulose fibrils in wood cell walls of other species (Table 2). On the other hand, various cellulose preparations exhibit crystalline regions with a great variety of sizes (Table 1), generally much larger than in the wood cell wall.

It should be noted, however, that all the methods employed here have their specific limitations. TEM suffers from the difficult sample preparation and staining methods, and the scattering methods from the fact that they are indirect techniques. In addition, WAXS results may also be affected by imperfections of the cellulose crystals. Altogether the overall agreement of all three techniques now establishes the existence of an ECF in *Picea abies*.

Acknowledgment. This work was supported by Fonds zur Förderung der wissenschaftlichen Forschung, FWF Project P10729-BIO.

References and Notes

(1) Heyn, A. N. *J. Appl. Phys.* **1955**, *5*, 519–526.
(2) Heyn, A. N. *J. Appl. Phys.* **1955**, *9*, 1113–1120.
(3) Blackwell, J.; Kolpak, F. J. *Macromolecules* **1975**, *8*, 322–326.
(4) Fink, H.-P.; Hofmann, D.; Purz, H. J. *Acta Polym.* **1990**, *41*, 131–137.
(5) Jakob, H. F.; Fratzl, P.; Tschegg, S. E. *J. Struct. Biol.* **1994**, *113*, 13–22.
(6) Fengel, D. *Holzforschung* **1978**, *32*, 37–44.
(7) Reimer, L. *Elektronenmikroskopische Untersuchungs- und Präparationsmethoden*; Springer-Verlag: Berlin, Heidelberg, New York, 1967.
(8) Robinson, D. G.; Ehlers, U.; Herken, R.; Herrmann, B.; Mayer, F.; Schürmann, F.-W. *Methods of Preparation for Electron Microscopy* Springer-Verlag: Berlin, Heidelberg, 1987.
(9) Wegener, G. *Papier* **1974**, *11*, 478–486.
(10) Spurr, A. R. *J. Ultrastruct. Res.* **1969**, *26*, 31–43.
(11) Gardner, K. H.; Blackwell, J. *Biopolymers* **1974**, *13*, 1975–2001.
(12) Azaroff, L. *Elements of X-ray Crystallography*; McGraw-Hill Book Co.: New York, 1968.
(13) Heyn, A. N. *J. Ultrastruct. Res.* **1969**, *26*, 52–68.
(14) Fengel, D.; Wegener, G. *Wood Chemistry, Ultrastructure, Reactions*; De Gruyter: Berlin, New York, 1984.
(15) Nomura, T. *Mokuzai Gakkaishi* **1992**, *6*, 533–542.
(16) Hearle, J. W. S. *J. Polym. Sci.* **1958**, *28*, 432–435.
(17) Fink, H.-P.; Fanter, D.; Phillip, B. *Acta Polym.* **1985**, *36*, 1–8.
(18) Scallan, A. M. *Text. Res. J.* **1971**, *41*, 647–653.
(19) Hindeleh, A. M.; Johnson, D. J. *Polymer* **1972**, *13*, 423–430.
(20) Haase, J.; Hosemann, R.; Renwanz, B. *Kolloid.-Z. Z. Polym.* **1973**, *251*, 871–875.
(21) Haase, J.; Hosemann, R.; Renwanz, B. *Colloid Polym. Sci.* **1974**, *252*, 712–717.
(22) Boylston, E. K.; Hebert, J. J. *J. Appl. Polym. Sci.* **1980**, *25*, 2105–2107.
(23) Nishimura, H.; Okano, T.; Asano I. *Mokuzai Gakkaishi* **1982**, *28*, 659–668.
(24) Fengel, D.; Jakob, H. F.; Strobl, C. *Holzforschung*, in press.
(25) Nomura, T.; Yamada, T. *Wood Res.* **1972**, *52*, 1–12.

MA950514W